Original article

Crosstalk of TNF-α, IFN-γ, NF-kB, STAT1 and redox signaling in lipopolysaccharide/D-galactosamine/dimethylsulfoxide-induced fulminant hepatic failure in mice

Abdulrazaq Alanazi [a], Mahmoud N. Nagi [a], Dhafer Y. Alhareth [a], Mohammed A Al-Hamamah [a], Mohamed A Mahmoud [a], Sheikh F. Ahmad [a], Mushtaq A. Ansari [a], Ahmed Nadeem [a], Saleh A. Bakheet [a], Gamaleldin I. Harisa [b], Sabry M. Attia [a,*]

[a] Department of Pharmacology and Toxicology, College of Pharmacy, King Saud University, KSA
[a] Department of Pharmaceutics, College of Pharmacy, King Saud University, KSA

ABSTRACT

Purpose: The clinical study of fulminant hepatic failure is challenging due to its high mortality and relative rarity, necessitating reliance on pre-clinical models to gain insight into its pathophysiology and develop potential therapies.
Methods and Results: In our study, the combination of the commonly used solvent dimethyl sulfoxide to the current-day model of lipopolysaccharide/D-galactosamine-caused fulminant hepatic failure was found to cause significantly greater hepatic damage, as indicated by alanine aminotransferase level. The effect was dose-dependent, with the maximum increase in alanine aminotransferase observed following 200 μl/kg dimethyl sulfoxide co-administration. Co-administration of 200 μl/kg dimethyl sulfoxide also remarkably increased histopathological changes induced by lipopolysaccharide/D-galactosamine. Importantly, alanine aminotransferase levels and survival rate in the 200 μl/kg dimethyl sulfoxide co-administration groups were both greater than those in the classical lipopolysaccharide/D-galactosamine model. We found that dimethyl sulfoxide co-administration aggravated lipopolysaccharide/D-galactosamine-caused liver damage by stimulating inflammatory signaling, as indicated by tumor necrosis factor alpha (TNF-α), interferon gamma (IFN-γ), inducible nitric oxide synthase (iNOS), and cyclooxygenase-2 (COX-2) levels. Further, nuclear factor kappa B (NF-kB) and transcription factor activator 1 (STAT1) were upregulated, as was neutrophil recruitment, indicated by myeloperoxidase activity. Hepatocyte apoptosis was also increased, and greater nitro-oxidative stress was noted, as determined based on nitric oxide, malondialdehyde, and glutathione levels.
Conclusion: Co-treatment with low doses of dimethyl sulfoxide enhanced the lipopolysaccharide/D-galactosamine-caused hepatic failure in animals, with higher toxicity and greater survival rates. The current findings also highlight the potential danger of using dimethyl sulfoxide as a solvent in experiments involving the hepatic immune system, suggesting that the new lipopolysaccharide/D-galactosamine/dimethyl sulfoxide model described herein could be used for pharmacological screening with the goal to better understand hepatic failure and evaluate treatment approaches.

* Corresponding author.
E-mail address: attiasm@ksu.edu.sa (S.M. Attia).

1. Introduction

Fulminant hepatic failure (FHF) is a life-threatening disease recognized by severe liver inflammation, including the increased release of inflammatory cytokines, reduced protein synthesis, and reduced detoxification, resulting in encephalopathy (Sass and Shakil 2005). FHF can have various causes, such as autoimmune hepatitis, Wilson's disease, and Hepatitis B infection, with viral- or toxin-induced FHF being most common. No curative treatment

for FHF exists, apart from liver replacement (Sass and Shakil 2005). While systemic inflammation is known to underpin FHF initiation and progression, the specific molecular mechanisms at play remain unclear. Understanding these is essential for the development of novel therapeutic medications.

Animal models enable the investigation of pathological mechanisms involved in FHF, facilitating the subsequent clinical translation of findings. Approaches for the induction of pre-clinical FHF models can be classified into immunogenic, surgical, or pharmacological. A number of pharmacological models have been investigated. Among the widely used agents are D-galactosamine (D-GalN), carbon tetrachloride, and acetaminophen (Hefler et al., 2021). D-GalN is an amino sugar derived from galactose and induces toxicity through depleting the uridine intracellular stores, which is required for RNA synthesis, thus resulting in UDP-galactosamine accumulation. This also deprives the cells of UDP-galactose, uridine derivative, and UDP-glucose, which are necessary for the synthesis of glycogen, in addition to altering intracellular calcium homeostasis, with major implications for energy metabolism, organelles, membranes, as well as nucleic acid and protein synthesis.

Within the liver, the innate immune system is the initial line of defenses against gut-derived lipopolysaccharide (LPS; bacterial toxin) and plays a critical role in the regulation of liver homeostasis (Robinson et al., 2016). The liver is specifically enriched in natural killer cells (NK), Kupffer cells, and natural killer T cells (NKT). These play a main role in killing off microorganisms. Pathogen-associated molecular patterns such as LPS, can recognize and activate pattern recognition receptors on specific antigen-presenting cells, such as Kupffer cells. In severe cases, activated Kupffer cells release several mediators, such as tumor necrosis factor alpha (TNF-α), which leads to neutrophil infiltration that can initiate the inflammatory response and subsequent liver injury (Triantafyllou et al., 2018). Additionally, activated NKT cells exert their actions via the release of the proinflammatory cytokines interferon gamma (IFN-γ) and TNF-α, whereas stimulated NK cells release IFN-γ (Tacke et al., 2009).

Mice are comparatively resistant to high LPS doses, which may induce death because of hypotensive shock, but do not lead hepatic injury. Nevertheless, D-GalN co-administration sensitized mice to LPS, leading to FHF (Galanos et al., 1979). The LPS/D-GalN combination model can induce FHF within a few hours, having become one of the most common experimental murine models of FHF for the study of novel therapeutic tools (Farghali et al., 2016, Maes et al., 2016). The sequential events that occur during FHF induction in this model are as follows: First, LPS binds to toll-like receptor 4 (TLR4) expressed on Kupffer cells and rapidly stimulates the expression cytokines, especially TNF-α, within a few hours (Schlayer et al., 1988). Second, TNF-α is a powerful neutrophil activator, and cell death mainly depends on reactive oxygen species formation by neutrophils, which induces intracellular oxidative stress in target cells (Jaeschke and Smith 1997). Third, TNF-α causes the expression of various adhesion molecules on sinusoidal endothelial cells, some of which are important for the extravasation and cytotoxicity of neutrophils (Jaeschke and Hasegawa 2006). Fourth, in the LPS/D-GalN model, secreted TNF-α primarily leads to hepatocyte apoptosis via TNF receptor 1 and caspase activations (Jaeschke et al., 1998). TNF-α produced by LPS-activated Kupffer cells can result in the survival or death of hepatocytes, depending on the signaling complex recruited to the receptor. The binding of TNF-α to its receptor stimulates the nuclear factor kappa B (NF-κB) pathway, causing the induction of antiapoptotic and proinflammatory proteins that provide survival signals and thus minimize hepatocyte death. Upon activation of the TNF receptor, NF-κB is activated, driving the transcription of antiapoptotic and proinflammatory genes (Liedtke and Trautwein 2012).

Nevertheless, high-dose D-GalN administration depletes cellular UTP pools and prevents RNA synthesis in liver cells for many hours. Transcription halts antiapoptotic gene expression, thus allowing signaling to proceed to caspase activation and subsequent DNA fragmentation (Maes et al., 2016).

Dimethyl sulfoxide (DMSO) is an amphiphilic molecule, meaning it has both lipophilic and hydrophilic characteristics, which makes it a suitable solvent for drugs and chemicals with low water solubility. DMSO is usually considered a relatively inert solvent, and its underappreciated effect may lead to the misinterpretation of experimental results. In many experimental studies, DMSO has been observed to have a wide-range of pharmacological effects that can be of relevance in the study of several pathological conditions. Importantly, DMSO can induce adverse biological effects (Jacob and Herschler 1986). An earlier report demonstrated the toxic effect of DMSO on NKT and NK cells *in vivo*, as indicated by the increased levels of proinflammatory cytokine IFN-γ (Masson et al., 2008). Therefore, we hypothesized that DMSO will exacerbate FHF induced by lower doses of the current LPS/D-GalN model through the exaggerated effect of the proinflammatory cytokines IFN-γ and TNF-α on hepatocytes, which could provide a modified and sensitive FHF model.

Numerous combinations of D-GalN and LPS have been applied to establish FHF. The most widely used combination is 50 μg/kg LPS and 800 mg/kg D-GalN. Although this 50 μg/800 mg combination can generate FHF within a few hours, it is accompanying with a high mortality rate. In contrast, the combination of 10 μg/kg LPS with 400 mg/kg D-GalN induces mild non-lethal hepatitis (Farghali et al., 2009, Farghali et al., 2016). LPS/D-GalN-caused-FHF is primarily mediated by Kupffer cells and NK cells, with IFN-γ and TNF-α as the decisive mediators that cause hepatic apoptosis. DMSO has been observed to elevate IFN-γ gene expressions in NK cells *in vivo* (Masson et al., 2008).

In the present investigation, we used LPS/D-GalN (10 μg/kg/400 mg/kg) in combination with DMSO to evaluate whether DMSO would aggravate FHF caused by lower doses of the current-day LPS/D-GalN model through the upregulation of proinflammatory cytokines TNF-α, and IFN-γ which could result in a modified and superior FHF model. We present an improved model of LPS/D-GalN-induced FHF achieved through the use of a lower dose of LPS/D-GalN (10 μg/kg/400 mg/kg) and the addition of a minor dose of DMSO (200 μl/kg) to develop higher toxicity and improve survival rate as compared to the classic LPS/D-GalN model (50 μg/kg/800 mg/kg). We consider that this model would be of use for understanding the molecular pathophysiology of FHF as well as for the pharmacological screening of potential FHF therapies.

2. Materials and methods

2.1. Mice

Male Swiss albino mice aged 9–12 weeks and weighing 19–26 g were used. The mice were acquired from the Animal Center of King Saud University, Pharmacy College, Riyadh, KSA. All mice were allowed to acclimatize in clean plastic cages (6 mice/plastic cage) inside a well-ventilated room before investigations. Animals were maintained in a well-conditioned animal house, with standard food and drinking water *ad libitum*, under a controlled atmosphere of humidity (40–60 %) and temperature (18–23 °C), with an alternating 12 light/12 h dark cycle. Once blood and liver samples were collected, the carcass were placed in appropriate colored opaque plastic bags which then were disposed according to protocol followed by the committee for prevention of chemical and biological pollution at King Saud University. All investigational processes

were carried out after approval from The Animal Care and Research Committee of the College of Pharmacy, King Saud University (KSU-SE-21–27), and all mice received humane care, consistent with NIH guidelines.

2.2. Experimental protocol

For the dose–response experiments, the mice were randomized into eight groups of 10 mice each. Different doses of DMSO (100, 200, and 400 μl/kg) were administered intraperitoneally directly after the LPS/D-GalN (10 μg/kg/ 400 mg/kg) injection. DMSO, LPS/ and D-GalN were obtained from Sigma-Aldrich (St. Louis, MO, USA). A saline-treated control group was also included. The tested doses of DMSO are non-toxic well tolerated by mice (LD_{50} = 6.2 mL/ kg, when applied intraperitoneally) (Bartsch et al., 1976). The doses of LPS and D-GalN were based on earlier published investigations (Farghali et al., 2016). Six hours after DMSO and/or LPS/D-GalN injection, the animals were euthanized by cervical dislocation after intraperitoneal administration of 50 mg/kg pentobarbital. Blood samples were withdrawn from the heart, and sera were separated for the assessment of liver injury based on the serum levels of alanine aminotransferase (ALT) measured using a diagnostic kit (Teco Diagnostics, Anaheim, CA). Administration of LPS/D-GalN resulted in a statistically significant rise in ALT activity as compared to that in untreated control mice. Co-administration of DMSO with LPS/D-GalN caused in a significant elevation in LPS/D-GalN hepatic injury in a dose-dependent manner, with the maximum increase in ALT activity observed with 200 μl/kg DMSO co-administration (Fig. 1). Based on these results, 200 μl/kg DMSO was chosen to explore the mechanisms underlying this aggravating effect.

For the main investigation, animals were randomly separated into four groups: the first group was administrated saline only, the second group received DMSO (200 μl/kg), the third group was administered LPS/D-GalN (10 μg/kg/ 400 mg/kg), and the fourth group was administered a mixture of LPS/D-GalN (10 μg/ kg/ 400 mg/kg) and DMSO (200 μl/kg). Animals were sacrificed 2 or 6 h following LPS/D-GalN and DMSO injection, where after liver and blood samples were collected. A group of mice injected with classical doses of LPS/D-GalN (50 μg/ kg/ 800 mg/kg) was also included to compare liver injury and mortality rates. For the survival test, mice in a separate ex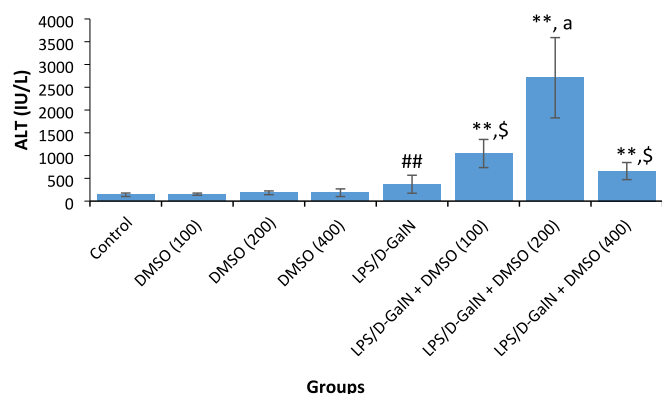periment were treated as in the main study, then animals were monitored every 2 h for 4 days, and dead mice were recorded.

2.3. Serum and liver sampling

Sera were extracted from withdrawn cardiac blood via centrifugation and then used fresh or frozen at −80 °C until use. Excised liver tissues were washed twice with ice-cold normal saline and processed for histopathology or stored at −80 °C until use in other assays. Livers were plotted dry on filter papers, weighed, homogenized in phosphate-buffered saline or in an appropriate buffer (100 mg/ml), and centrifuged at 4 °C. Supernatant protein concentrations were assessed using a BCA protein assay kit (Santa Cruz Biotechnology, Inc., USA) with BSA as the standard, following manufacturer instructions.

2.4. Biochemical analysis

Serum ALT, AST, bilirubin, albumin, urea, TNF-α and IFN-γ concentrations were assessed using ELISA kits, following manufacturer's instruction. Liver reduced glutathione (GSH) level was assessed using 5,5′-dithiobis (2-nitrobenzoic acid) based on the methods of Ellman (Ellman 1959), with GSH as the standard, as previously described (Attia et al., 2009). Lipid peroxidation in the hepatic homogenate was determined using a method described earlier (Ohkawa et al., 1979), based on one of the end-product of this process, thiobarbituric acid reactive substances (TBARS). Since 99 % of TBARS are malondialdehyde (MDA), lipid peroxide levels were evaluated from a standard curve using 1,1,3,3-tetra-methoxy-propane, as described earlier (Attia 2008). Nitrate/nitrite (NOx) in hepatic samples was evaluated as nitrite based on the technique illustrated by Miranda et al. (Miranda et al., 2001), as previously described (Harisa et al., 2014). Hepatic caspase-3 activity was assessed by the Caspase-3/CPP32 colorimetric assay kits (BioVision, Mountain View, CA, USA) according to the manufacturer's protocol, as previously described (Bakheet et al., 2011, Saquib et al., 2012). Myeloperoxidase (MPO) activity in liver homogenates was assessed using an adaptation of the protocol described by Bradley et al. (Bradley et al., 1982).

2.5. Real-Time PCR

TRIzol reagent was applied to extract total RNA form excised livers, according to the manufacturer's instructions. The quantity and quality of the eluted RNA were evaluated with a NanoDrop 8000 spectrophotometer by measuring the absorbance at 260 nm and the 260:280 nm ratio, respectively. cDNA was produced via reverse transcription using a High-Capacity cDNA Archive Kits (Applied Biosystems, CA, USA) (Attia et al., 2013). Real-time polymerase chain reaction was carried out using commercially available primers for mouse cyclooxygenase-2 (COX-2), inducible nitric oxide synthase (iNOS), and GAPDH on a 7500 Fast Real-Time PCR System (Applied Biosciences), as previously described (Ahmad et al., 2015, Al-Hamamah et al., 2019). The primers that were used in this investigation are shown in Table 1 (Alanazi

Fig. 1. DMSO aggravates LPS/D-GalN increased serum ALT activity. Data shown as mean ± SD (N = 6). Different doses of DMSO (100, 200, and 400 μl/kg) was administered intraperitoneally following LPS/D-GalN (10 μg/kg/400 mg/kg) injection. Six hours following injection, blood samples were withdraw for evaluation of serum levels of ALT activity. **$P < 0.01$ versus control animals and [a]$P < 0.05$ versus LPS/D-GalN (10/400) exposed animals (Kruskal-Wallis test followed by Dunn's test for multiple comparisons). [$]$P < 0.01$ versus LPS/D-GalN exposed animals and ##$P < 0.01$ versus control animals (Mann-Whitney U test). LPS = lipopolysaccharide, D-GalN = D galactosamine and DMSO = dimethyl sulfoxide.

Table 1
Mice primer sequences used for RT- PCR.

Gene	Primer sequences
COX-2	F: 5′-CAT TCT TTG CCC AGC ACT TCA C-3′
	R: 5′-GAC CAG GCA CCA GAC CAA AGA C-3′
iNOS	F: 5′-CCT GGT ACG GGC ATT GCT-3′
	R: 5′-GCT CAT GCG GCC TCC TTT-3′
GAPDH	F: 5′-TGA AGC AGG CAT CTG AGG G-3′
	R: 5′-CGA AGG TGG AAG AGT GGG AG-3′

et al., 2017). Relative gene expression was calculated as per the $2^{-\Delta\Delta CT}$ method (Livak and Schmittgen 2001). Data are shown as the fold-changes in gene expressions normalized to the reference GAPDH gene.

2.6. Western blot analysis

Liver tissues were homogenized in the RIPA lysis buffer (150 mM NaCl, 0.1 % SDS, 1 % Nonidet P-40, 20 mM Tris, 0.5 % sodium deoxycholate and 1 mM EDTA) containing the protease inhibitors at 4 °C. The lysates were kept on ice for 1 h with sporadic vortexing every 10 min and then centrifuged at 16000 rpm for 10 min at 4 °C. Total protein in the supernatant RIPA-soluble fraction was determined using a BCA protein assay kits (Santa Cruz Biotechnology, Inc., USA), following the manufacturer's instruction. Supernatant protein (25 μg) was boiled in equal amount of 2x Laemmli sample buffer (65.8 mM Tris-HCl, pH 6.8, 26.3 % (w/v) glycerol, 2.1 % SDS, 0.01 % bromophenol blue and 5 % β-mercaptoethanol) for 5 min and then pipetted into 10 % SDS poly-acrylamide gel. Following electrophoresis, protein samples were transferred onto methanol pre-soaking PVDF membrane in a transfer buffer (25 mM Tris-HCl, 25 % methanol, and 192 mM glycine) and blotted with primary antibodies against NF-κB, Tyr701-phosphorylated transcription factor activator 1 (pSTAT1), total STAT1, and β-actin (Santa Cruz Biotechnology, US) diluted to 1:5000, overnight. The nitrocellulose membranes were washed with wash buffer (0.1 % Tween-20 in TBS) and incubated with the 1:1000 dilution of horseradish peroxidase-conjugated secondary antibodies for 60 min at 25 °C, as previously described (Ahmad et al., 2017, Attia et al., 2017). Enhanced chemiluminescence (Amersham Pharmacia Biotech, NJ) was applied to picture the protein bands. The intensity of distinct bands was evaluated by densitometry (C-DiGit Blot Scanner, LI-COR Inc. USA) and normalized to that of the housekeeping gene β-actin.

2.7. Histopathological examination

Hepatic tissues were fixed in 10 % formalin solution for a minimum 48 h and used for further processing. The liver specimens were then sliced, and sections were used for histopathological assessments. Following routine automated processing, the histopathology slides containing the liver specimens were stained with hematoxylin and eosin (H & E) (Zoheir et al., 2015). The stained glass slides were investigated by an experienced histopathologist in the absence and presence of liver injury.

2.8. Statistics

Results are shown as the mean ± SD. The obtained data were first analyzed for normality and homogeneity of the mean using the Kolmogorov-Smirnov and Bartlett's tests, respectively. Data were analyzed using parametric, Student's *t*-test, and one-way ANOVA followed by Tukey-Kramer test for multiple comparisons or non-parametric, Mann-Whitney *U* test, and Kruskal-Wallis test followed by Dunn's test for multiple comparison. All analyses were performed using Graph Pad InStat software. Differences were considered significant if $P < 0.05$.

3. Results

3.1. DMSO exacerbates the LPS/D-GalN-induced increase in ALT

Fig. 1 shows the influence of different concentrations of DMSO on the serum ALT activity at 6 h in LPS/D-GalN-treated and untreated mice. Administration of a single dose of LPS/D-GalN

(10 μg/kg/ 400 mg/kg) resulted in a significant rise in ALT activity compared with control mice. We did not detect any significant differences in serum ALT activity between animals receiving different doses of DMSO. Administration of DMSO (100, 200 and 400 μl/kg) together with LPS/D-GalN significantly increased LPS/D-GalN toxicity at all tested doses. The highest ALT activity was observed with 200 μl/kg DMSO when compared to that in the LPS/D-GalN-injected mice. We therefore decided to use 200 μl/kg DMSO in subsequent experiments exploring the underlying mechanisms of this exacerbated hepatotoxic effect.

3.2. DMSO exacerbates LPS/D-GalN-induced liver injury and improves survival rate

In the classical model of LPS/D-GalN (50 μg/kg/ 800 mg/kg), the activity of mice was markedly decreased, and a great number of short-term deaths were noted. Clinical assessment revealed that death was preceded by progressive hepatic encephalopathy characterized by an impaired response to painful stimuli, weakened head support, deteriorated righting reflex, and lethargy. The mice soon developed hepatic coma, which lasted for approximately 2 h before animal death. These data were in line with the clinico-pathological characteristics of FHF, indicating that the FHF mouse model was successfully constructed. As shown in Table 2 and Fig. 2, LPS/D-GalN injection significantly elevated serum bilirubin, urea, ALT and AST levels, while decreasing serum albumin levels. Co-administration of 200 μl/kg DMSO and LPS/D-GalN (10 μg/kg/ 400 mg/kg) markedly worsened these parameters. Meanwhile, administration of DMSO alone (200 μl/kg) resulted in non-significant alterations in the parameters compared to their values in untreated control mice. At six hours following LPS/D-GalN treatment, the mortality rate in the classical model of LPS/D-GalN (50 μg/kg/ 800 mg/kg), was 37.5 %, and all animals died within 10 h, whereas in the animals receiving LPS/D-GalN (10 μg/kg/ 400 mg/kg) with or without 200 μl/kg DMSO, the mortality rate was approximately 14 % (Fig. 2). After LPS/GalN (50 μg/kg/800 mg/kg) injection, the animals began to die within 5 h, and the death rate reached 100 % at 10 h. In contrast, animals treated with LPS/D-GalN (10 μg/kg/ 400 mg/kg) with or without DMSO started to die at 6 h and co-administration of 200 μl/kg DMSO was remarkably able to maintain the survival rate of animals treated with LPS/D-GalN (10 μg/kg/ 400 mg/kg). All mice treated with LPS/D-GalN (10 μg/kg/ 400 mg/kg) with or without 200 μl/kg DMSO died within 3 days (Fig. 3), following the development of hepatic encephalopathy and a period of hepatic coma that lasted 2 h on average before death. Blood drawn from animals was not included in the survival statistics.

3.3. DMSO increases proinflammatory cytokine production in LPS/D-GalN-injected mice

LPS-induced proinflammatory cytokine production increases local inflammation and immune cell infiltration, with subsequent liver damage. Figs. 4 and 5 show the effect of 200 μl/kg DMSO on the serum levels of proinflammatory cytokines TNF-α and IFN-γ in LPS/D-GalN (10 μg/kg/ 400 mg/kg)-treated and control animals. We did not observe significant changes in the levels of these cytokines in DMSO-treated mice. TNF-α and IFN-γ were significantly elevated in LPS/D-GalN animals 2 h after injection compared to their levels in control animals. Co-treatment of DMSO with LPS/D-GalN resulted in an obvious elevation in TNF-α and IFN-γ levels when compared with LPS/D-GalN alone.

Table 2
Liver injury parameters in animals following LPS/D-GalN and DMSO injections.

Groups	Bilirubin (mg/dl)	Albumins (g/dl)	Blood urea (mg/dl)	AST activity (U/L)
Control	0.91 ± 0.27	3.15 ± 0.66	39.83 ± 7.57	139.12 ± 38.14
DMSO	0.90 ± 0.23	3.10 ± 0.80	42.33 ± 8.68	185.50 ± 41.90
LPS/D-GalN	2.66 ± 0.51**	1.90 ± 0.39**	95.50 ± 11.77**	371.00 ± 89.0*
LPS/D-GalN/DMSO	4.16 ± 0.52**,b	1.31 ± 0.41**,b	140.0 ± 16.11**,b	2708.0 ± 575**,b

Data shown as mean ± SD (N = 6). DMSO (200 µl/kg) was administered intraperitoneally following LPS/D-GalN (10 µg/kg/400 mg/kg) injection. Six hours following injection, blood were withdraw for measurements of serum levels of bilirubin, albumins, blood urea and AST activity. *$P < 0.05$ and **$P < 0.01$ versus control animals and b$P < 0.01$ versus LPS/D-GalN (10/400) exposed animals (ANOVA test followed by Tukey-Kramer test for multiple comparisons). LPS = lipopolysaccharide, D-GalN = D galactosamine and DMSO = dimethyl sulfoxide.
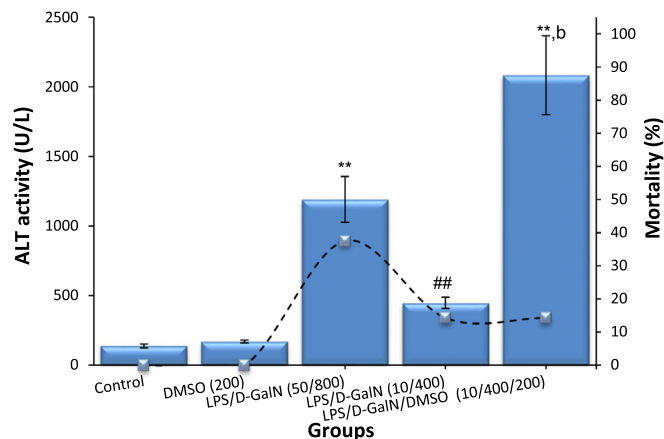

Fig. 2. DMSO aggravates LPS/D-GalN caused-liver injury as determined by ALT activity (blue bars) and reduces the mortality rate (dashed line). Data shown as mean ± SD (N = 6). DMSO (200 µl/kg) was administered intraperitoneally following LPS/D-GalN (10 µg/kg/400 mg/kg) injection. Six hours following injection, blood samples were withdraw for measurements of serum level of ALT activity. Mortality rate was wlso recorded during 6 h following treatment. **$P < 0.01$ versus control animals (Kruskal-Wallis test followed by Dunn's test for multiple comparisons). ##$P < 0.01$ versus control animals and b$P < 0.01$ versus LPS/D-GalN (10/400) exposed animals (Mann-Whitney U test). LPS = lipopolysaccharide, D-GalN = D galactosamine and DMSO = dimethyl sulfoxide.
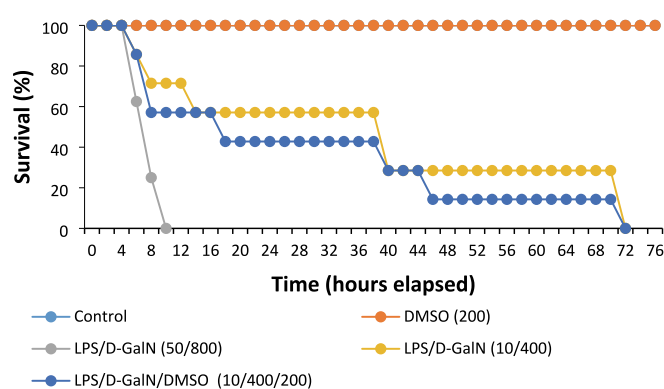

Fig. 3. DMSO co-administration improves the survival rate. DMSO (200 µl/kg) was administered intraperitoneally following LPS/D-GalN (10 µg/kg/400 mg/kg) injection. LPS = lipopolysaccharide, D-GalN = D galactosamine and DMSO = dimethyl sulfoxide.

3.4. DMSO stimulates LPS/D-GalN-caused NF-κB and STAT1 activations

The results of western blotting are presented in Fig. 6. Representative bands for each protein of interest and β-actin are shown in Fig. 6A. Since NF-κB is a master regulator of inflammatory responses to LPS, its expression was examined. As seen in Fig. 6B, animals treated with 200 µl/kg DMSO did not show any difference
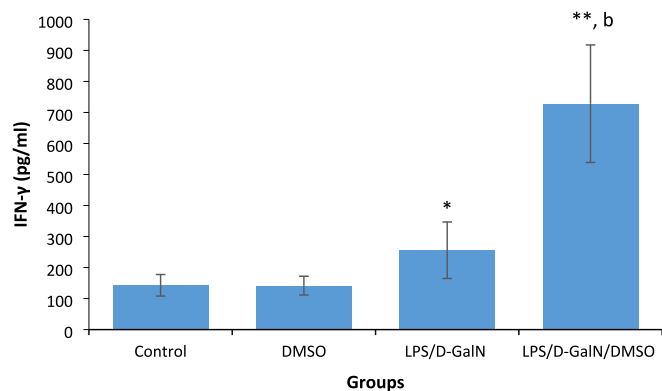

Fig. 4. DMSO increases the pro-inflammatory cytokine IFN-γ production in LPS/D-GalN treated animals. Data shown as mean ± SD (N = 6). DMSO (200 µl/kg) was administered intraperitoneally following LPS/D-GalN (10 µg/kg/400 mg/kg) injection. Two hours following injection, blood samples were withdraw for measurements of serum level of IFN-γ. *$P < 0.05$ and **$P < 0.01$ versus control animals (Kruskal-Wallis test followed by Dunn's test for multiple comparisons). b$P < 0.01$ versus LPS/D-GalN (10/400) exposed animals (Mann-Whitney U test). LPS = lipopolysaccharide, D-GalN = D galactosamine and DMSO = dimethyl sulfoxide.
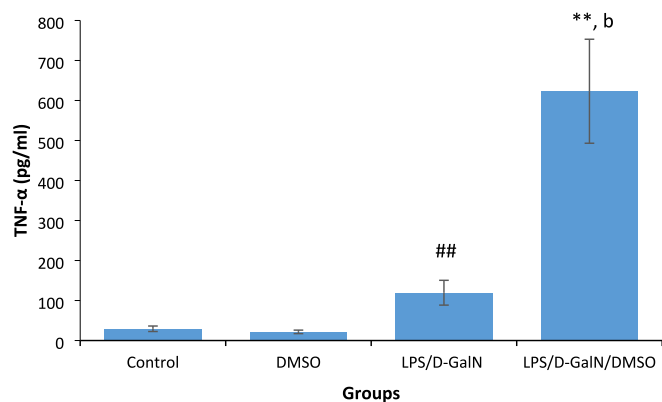

Fig. 5. DMSO increases pro-inflammatory cytokine TNF-α production in LPS/D-GalN treated animals. Data shown as mean ± SD (N = 6). DMSO (200 µl/kg) was administered intraperitoneally following LPS/D-GalN (10 µg/kg/400 mg/kg) injection. Two hours following injection, blood samples were withdraw for measurements of serum level of TNF-α. **$P < 0.01$ versus control animals (Kruskal-Wallis test followed by Dunn's test for multiple comparisons). ##$P < 0.01$ versus control animals and b$P < 0.01$ versus LPS/D-GalN (10/400) exposed animals (Mann-Whitney U test). LPS = lipopolysaccharide, D-GalN = D galactosamine and DMSO = dimethyl sulfoxide.

in NF-κB expression compared to untreated control animals. Cellular NF-κB levels were significantly upregulated in the hepatocytes of mice treated with LPS/D-GalN (10 µg/kg/ 400 mg/kg) when compared to untreated control mice hepatocytes. Co-treatment of
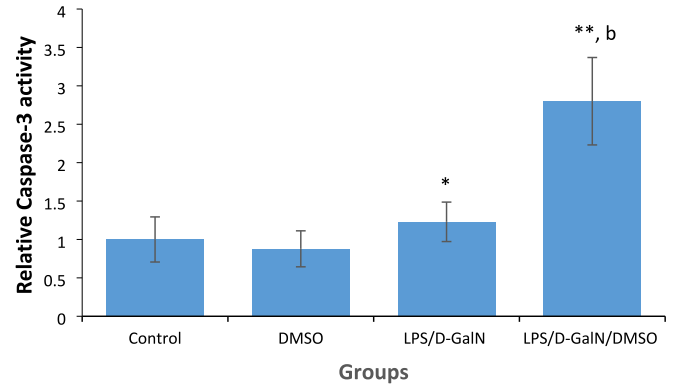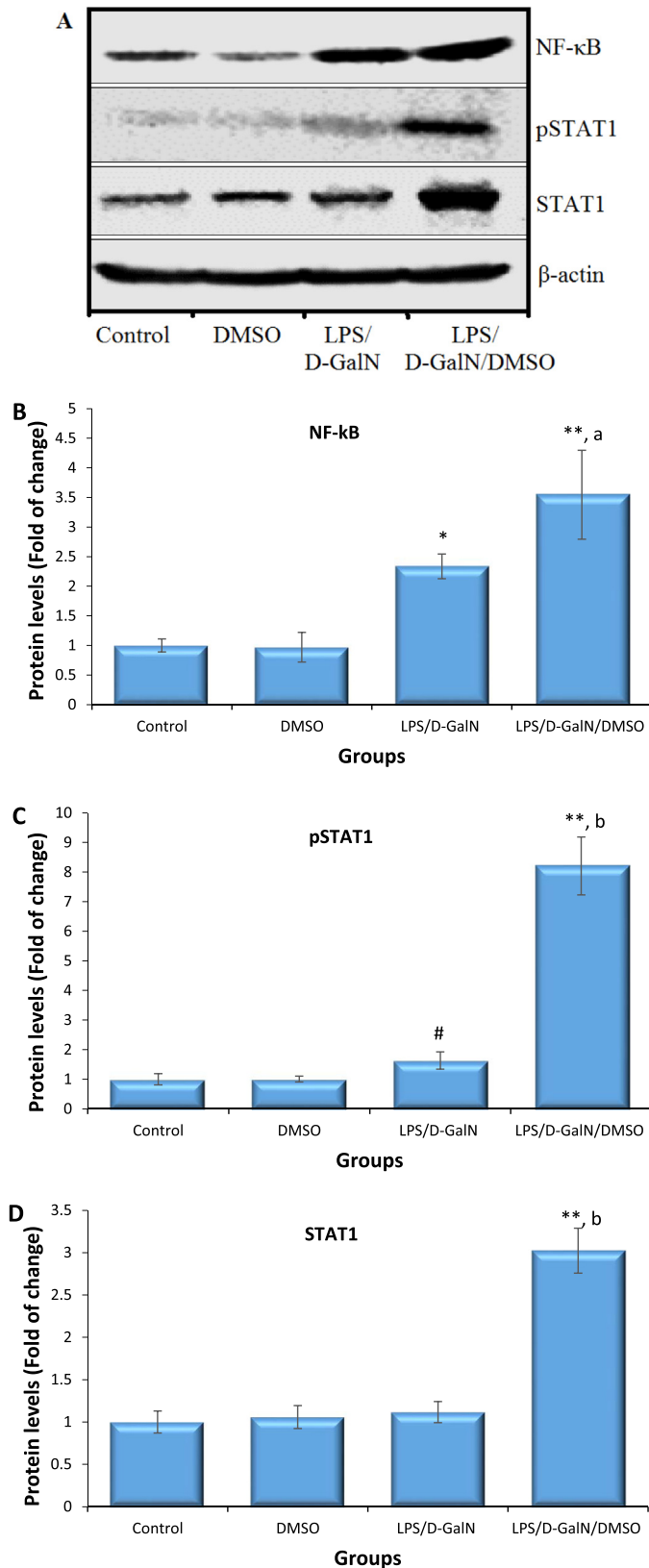
Fig. 7. DMSO increases LPS/ᴅ-GalN-caused hepatic cell apoptosis as determined by measuring caspase-3 activity. Data shown as mean ± SD (N = 6). DMSO (200 µl/kg) was administered intraperitoneally following LPS/ᴅ-GalN (10 µg/kg/400 mg/kg) injection. Six hours after injection, livers were isolated for measurements of caspase-3 activity. *$P < 0.05$ and **$P < 0.01$ versus control animals (ANOVA test followed by Tukey-Kramer test for multiple comparisons). [b]$P < 0.01$ versus LPS/ᴅ-GalN (10/400) exposed animals (Student *t*-test). LPS = lipopolysaccharide, ᴅ-GalN = D galactosamine and DMSO = dimethyl sulfoxide.

DMSO with LPS/ᴅ-GalN significantly upregulated NF-κB levels 2.7-fold compared to those in control mice and 2.28-fold compared to those in mice receiving LPS/ᴅ-GalN alone. Thus, co-administration of DMSO increased LPS/ᴅ-GalN-caused NF-κB levels in hepatocytes.

To understand the role of IFN-γ in hepatic damage in LPS/ᴅ-GalN/DMSO-caused FHF, the activation and expression of STAT1, a key transcription factor upregulated in response to IFN-γ, was determined. As shown in Fig. 6C, animals treated with 200 µl/kg DMSO did not show any difference in STAT1 tyrosine phosphorylation (p-STAT1) nor STAT1 protein expression, compared to untreated control animals. Administration of LPS/ᴅ-GalN (10 µg/kg/ 400 mg/kg) rapidly induced STAT1 tyrosine phosphorylation within 2 h. In contrast, STAT1 protein expression was not significantly elevated in the LPS/ᴅ-GalN treated mice. Co-treatment of DMSO with LPS/ᴅ-GalN resulted in a significant rise in STAT1 tyrosine phosphorylation by 8.2-fold compared to that in control mice and 5.02-fold compared to that in LPS/ᴅ-GalN-injected animals. STAT1 expression was slightly elevated in the LPS/ᴅ-GalN-caused FHF model, but this increase was not statistically significant. However, a clear upregulation of the STAT1 protein was found in the LPS/ᴅ-GalN/DMSO-treated mice (Fig. 6D).

3.5. DMSO increases LPS/ᴅ-GalN-caused hepatic apoptosis

Hepatic apoptosis is the major driver of the liver injury observed in FHF. LPS/ᴅ-GalN-caused liver apoptosis was assessed by measuring caspase-3 activation in livers. As presented in Fig. 7, animals treated with 200 µl/kg DMSO did not show any change in caspase-3 activity as compared to untreated control animals. The hydrolytic activity of caspase-3 towards DEVD p-NA was significantly increased 1.3-fold in the hepatocytes of mice admin-

Fig. 6. DMSO stimulates LPS/ᴅ-GalN-caused NF-κB, and STAT1 activation. Data shown as mean ± SD (N = 6). DMSO (200 µl/kg) was administered intraperitoneally following LPS/ᴅ-GalN (10 µg/kg/400 mg/kg) injection. Six hours following injection, liver tissues were isolated for measurements of NF-κB activation. **A**, Representative image of the western blotting for each examined protein as well as the β-actin housekeeping gene. Graph donating the difference in expressions of NF-κB (B), pSTAT1 (C) and STAT1 protein (D). *$P < 0.05$ and **$P < 0.01$ versus control animals and [a]$P < 0.05$ and [b]$P < 0.01$ versus LPS/ᴅ-GalN (10/400) exposed animals (ANOVA test followed by Tukey-Kramer test for multiple comparisons). [#]$P < 0.05$ versus exposed control animals (Student *t*-test). LPS = lipopolysaccharide, ᴅ-GalN = D galactosamine and DMSO = dimethyl sulfoxide.

istered LPS/ᴅ-GalN (10 μg/kg/ 400 mg/kg) when compared to that in hepatocytes from control mice. Co-injection of DMSO with LPS/ᴅ-GalN significantly increased caspase-3 activity 2.7-fold compared to that in control mice and 2.3-fold compared to that in LPS/ᴅ-GalN-administrated animals.

3.6. DMSO stimulates LPS/ᴅ-GalN-caused FHF by upregulating COX-2 expression

During inflammation, phosphorylated NF-κB drives the expressions of inflammatory enzymes, involving COX-2 and iNOS. As shown in Fig. 8, animals treated with 200 μl/kg DMSO did not exhibit any change in COX-2 expression compared to untreated control mice. LPS/ᴅ-GalN (10 μg/kg/ 400 mg/kg) treatment significantly increased COX-2 expression in the mouse liver 2 h after treatment, with COX-2 expression being significantly upregulated following DMSO co-administration as compared to that in control and LPS/ᴅ-GalN-injected animals, indicative of greater hepatic inflammation.

3.7. DMSO stimulates LPS/ᴅ-GalN-induced neutrophil infiltration

Neutrophil granules contain MPO, an enzyme that produces hypohalous acids with antimicrobial activity. MPO is a marker of neutrophil recruitment, with MPO activity providing a quantitative index of tissue neutrophil content and reflecting the proportion of neutrophils that migrate from blood into the liver during inflammation. As shown in Fig. 9, animals treated with 200 μl/kg DMSO did not show any change in MPO activity compared with untreated control animals. LPS/ᴅ-GalN (10 μg/kg/ 400 mg/kg) administration significantly increased MPO activity in mouse livers 6 h after treatment, and MPO activity was further enhanced following co-administration of DMSO with LPS/ᴅ-GalN when compared to activity levels in control and LPS/ᴅ-GalN-treated mice.

3.8. DMSO stimulates LPS/ᴅ-GalN-caused nitro-oxidative stress

The influence of DMSO (200 μl/kg) on LPS/ᴅ-GalN-caused nitro-oxidative stress was assessed by measuring the level hepatic iNOS, its product nitric oxide (NO), as well as GSH and MDA. As presented in Fig. 10, DMSO-treated mice did not display any changes in iNOS mRNA levels at the tested dose. At 2 h after LPS/ᴅ-GalN
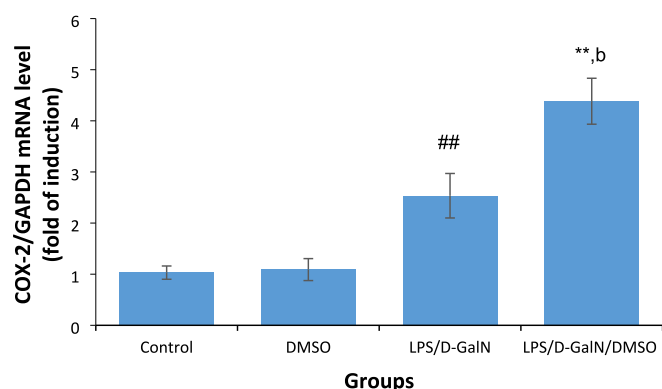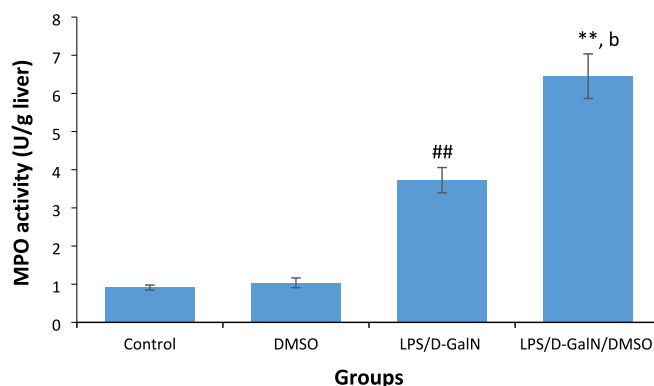

Fig. 9. DMSO stimulates LPS/ᴅ-GalN-caused neutrophil infiltration as determined by measuring Myeloperoxidase (MPO) activity. Data shown as mean ± SD (N = 6). DMSO (200 μl/kg) was administered intraperitoneally following LPS/ᴅ-GalN (10 μg/kg/400 mg/kg) injection. Six hours following injection, livers were isolated for measurements of MPO activity. **$P < 0.01$ versus control animals and $^b P < 0.01$ versus LPS/ᴅ-GalN (10/400) exposed animals (Kruskal-Wallis test followed by Dunn's test for multiple comparisons). $^{##}P < 0.01$ versus control animals (Mann-Whitney U test). LPS = lipopolysaccharide, ᴅ-GalN = D galactosamine and DMSO = dimethyl sulfoxide.
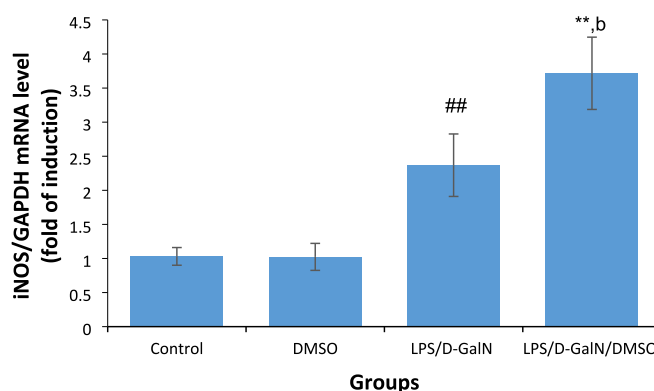

Fig. 10. DMSO stimulates LPS/ᴅ-GalN-caused FHF by increasing iNOS expression. Data shown as mean ± SD (N = 6). DMSO (200 μl/kg) was administered intraperitoneally following LPS/ᴅ-GalN (10 μg/kg/400 mg/kg) injection. Two hours following injection, livers were isolated for measurements of iNOS levels. **$P < 0.01$ versus control animals (Kruskal-Wallis test followed by Dunn's test for multiple comparisons). $^{##}P < 0.01$ versus control animals and $^b P < 0.01$ versus LPS/ᴅ-GalN (10/400) exposed animals (Mann-Whitney U test). LPS = lipopolysaccharide, ᴅ-GalN = D galactosamine and DMSO = dimethyl sulfoxide.

(10 μg/kg/400 mg/kg) treatment, the mRNA expressions of iNOS in liver tissue was significantly upregulated, and this upregulation was markedly enhanced 3.7-fold in LPS/ᴅ-GalN/DMSO-treated mice when compared to untreated control animals and 1.6-fold compared to that in mice receiving LPS/ᴅ-GalN treatment alone. As presented in Fig. 11, NOx production was not altered in mice treated with DMSO alone. Conversely, NOx production was significantly induced by LPS/ᴅ-GalN (10 μg/kg/ 400 mg/kg) in the mouse liver after 6 h of treatment. Co-administration of DMSO with LPS/ᴅ-GalN resulted in a significant increase in NOx production compared with the untreated control mice and the LPS/ᴅ-GalN group.

Similarly, hepatic MDA level was not altered in DMSO-treated animals and were significantly increased in LPS/ᴅ-GalN (10 μg/kg/ 400 mg/kg)-treated mice. Co-treatment with DMSO significantly increased MDA levels relative to those after injection of LPS/ᴅ-GalN alone (Fig. 12). Additionally, liver GSH level was not significantly different in DMSO-injected mice compared to those receiving the vehicle control. In contrast, GSH levels in LPS/ᴅ-GalN (10 μg/kg/400 mg/kg)-treated mice were significantly

Fig. 8. DMSO stimulates LPS/ᴅ-GalN-caused FHF by increasing COX-2 expression. Data shown as mean ± SD (N = 6). DMSO (200 μl/kg) was administered intraperitoneally following LPS/ᴅ-GalN (10 μg/kg/400 mg/kg) injection. Two hours following injection, livers were isolated for measurements of COX-2 levels. **$P < 0.01$ versus control animals (Kruskal-Wallis test followed by Dunn's test for multiple comparisons). $^{##}P < 0.01$ versus control animals and $^b P < 0.01$ versus LPS/ᴅ-GalN (10/400) exposed animals (Mann-Whitney U test). LPS = lipopolysaccharide, ᴅ-GalN = D galactosamine and DMSO = dimethyl sulfoxide.
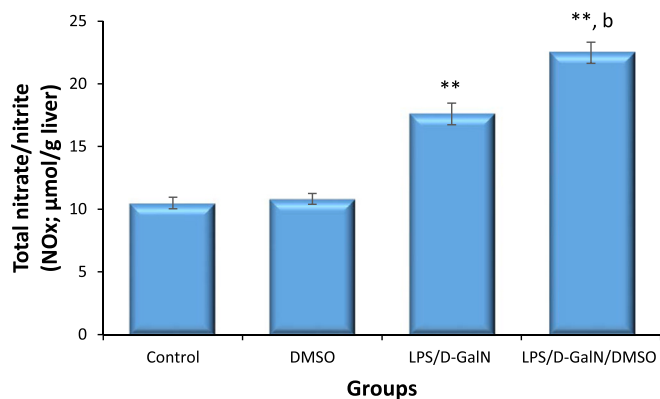
Fig. 11. **DMSO stimulates LPS/ᴅ-GalN-caused nitrosative stress as determined by NOx production.** Data shown as mean ± SD (N = 6). DMSO (200 µl/kg) was administered intraperitoneally following LPS/ᴅ-GalN (10 µg/kg/400 mg/kg) injection. Six hours following injection, livers were isolated for measurements of NOx production. **P < 0.01 versus control animals and ^{b}P < 0.01 versus LPS/ᴅ-GalN (10/400) exposed animals (ANOVA test followed by Tukey-Kramer test for multiple comparisons). LPS = lipopolysaccharide, ᴅ-GalN = D galactosamine and DMSO = dimethyl sulfoxide.

Fig. 13. **DMSO stimulates LPS/ᴅ-GalN-caused oxidative stress as determined by GSH levels.** Data shown as mean ± SD (N = 6). DMSO (200 µl/kg) was administered intraperitoneally following LPS/ᴅ-GalN (10 µg/kg/400 mg/kg) injection. Six hours following injection, livers were isolated for measurements of GSH levels. **P < 0.01 versus control animals and ^{b}P < 0.01 versus LPS/ᴅ-GalN (10/400) exposed animals (ANOVA test followed by Tukey-Kramer test for multiple comparisons). LPS = lipopolysaccharide, ᴅ-GalN = D galactosamine and DMSO = dimethyl sulfoxide.
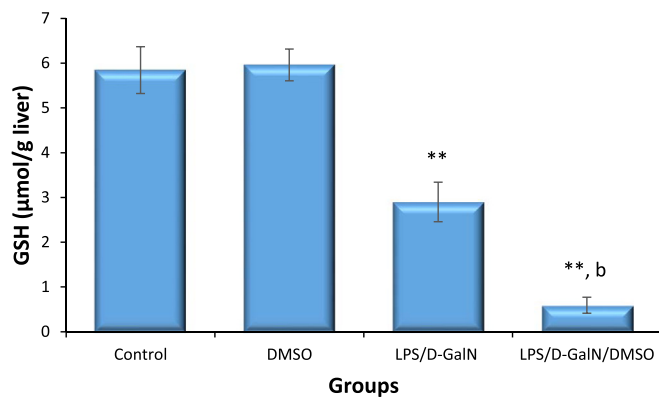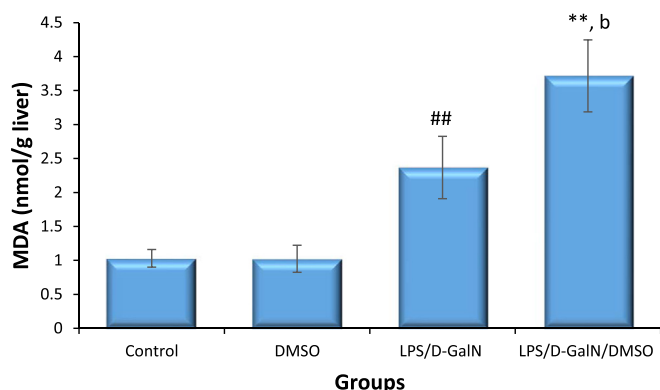

Fig. 12. **DMSO stimulates LPS/ᴅ-GalN-caused oxidative stress as determined by MDA levels.** Data shown as mean ± SD (N = 6). DMSO (200 µl/kg) was administered intraperitoneally following LPS/ᴅ-GalN (10 µg/kg/400 mg/kg) injection. Six hours following injection, livers were isolated for measurements of MDA levels. **P < 0.01 versus control animals (Kruskal-Wallis test followed by Dunn's test for multiple comparisons). ##P < 0.01 versus control animals and ^{b}P < 0.01 versus LPS/ᴅ-GalN (10/400) exposed animals (Mann-Whitney U test). LPS = lipopolysaccharide, ᴅ-GalN = D galactosamine and DMSO = dimethyl sulfoxide.
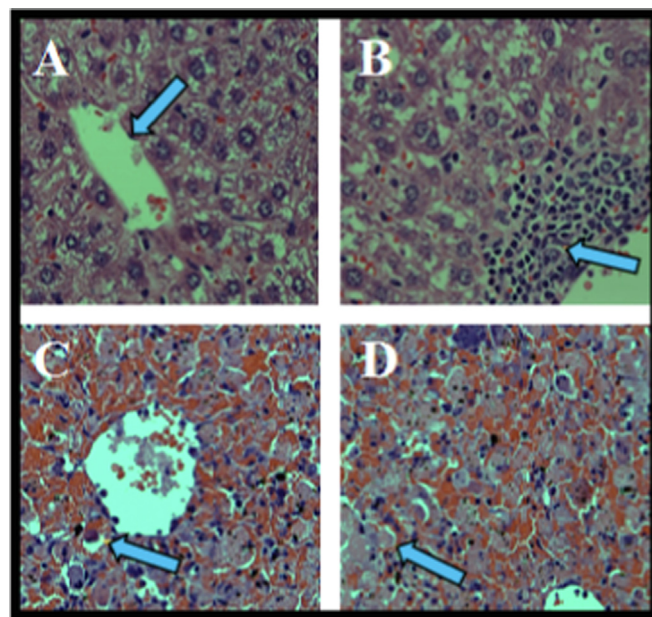
reduced compared to those in control mice (Fig. 13), and the LPS/ᴅ-GalN-induced reduction of GSH was profoundly increased by DMSO co-treatment and reduced to a level significantly different from those in the untreated control and LPS/ᴅ-GalN groups.

3.9. DMSO exacerbates LPS/ᴅ-GalN caused-histopathological changes

We found histopathological alterations at 6 h following LPS/ᴅ-GalN treatment, including hepatocyte necrosis around the central hepatic vein, congestion of hepatic sinusoids, marked apoptosis, and prominent cholestasis. Treatment with 200 µl/kg DMSO markedly increased histopathological changes in animals treated with LPS/ᴅ-GalN (10 µg/kg/ 400 mg/kg). DMSO plus LPS/ᴅ-GalN induced marked hepatic necrosis with markedly congested liver sinusoids, erythrocyte influx (hemorrhage), and apoptotic bodies accompanied by several inflamed portal tracts surrounded by extensive hepatocyte necrosis, when compared to control mice and those treated with LPS/ᴅ-GalN alone (Fig. 14).

Fig. 14. Histopathological examination of liver section six hours following DMSO (200 µl/kg) with and without LPS/ᴅ-GalN (10 µg/kg/400 mg/kg) injection. Liver sections were stained with eosin/hematoxylin stains (×400). In control animals (**A**), the liver tissues appear normal with central vein (arrow). In DMSO (200 µl/kg) treated animals (**B**), the liver tissues appear normal with the manifestation of an aggregate of lymphohistiocytic cells (arrowhead). In LPS/ᴅ-GalN injected animals (**C**), the section presenting hepatic necrosis around the central hepatic vein with councilman body formations (arrow). Marked congestion of hepatic sinusoids, apoptosis, and prominent cholestasis were also found. In DMSO (200 µl/kg) co-injected animals (**D**), extensive hepatic necrosis (arrowhead) with markedly congested liver sinusoids, apoptotic bodies, erythrocyte influxs (hemorrhage) and large numbers of inflammatory cells infiltrated were observed following DMSO co-treatment with LPS/ᴅ-GalN. LPS = lipopolysaccharide, ᴅ-GalN = D galactosamine and DMSO = dimethyl sulfoxide.

4. Discussion

The development of effective treatment for hepatic disease depends on the availability of representative model systems of hepatic injury. Animal models have been successfully employed for the study of pathophysiological mechanisms involved in hep-

atic disease, given that they are reproducible and can recapitulate hepatic failure events (Gama et al., 2022). In our preliminary experiment, we used a combination of DMSO and LPS/ᴅ-GalN (10 μg/kg/400 mg/kg) to test whether DMSO co-treatment can aggravate FHF in animals receiving LPS/ᴅ-GalN (10 μg/kg/ 400 mg/kg). High serum ALT levels in mice detected 6 h following LPS/ᴅ-GalN exposure clearly indicated LPS/ᴅ-GalN-caused FHF. A combination of LPS/ᴅ-GalN with different doses of DMSO was observed to cause a significantly higher dose-dependent increase in ALT than LPS/ᴅ-GalN administration alone, with the greatest increase observed following 200 μl/kg DMSO co-administration. In harmony with our data, administration of 250 μl/kg DMSO had a significant impact on acetaminophen-induced hepatic injury in mice (Masson et al., 2008). Importantly, the high dose of DMSO (400 μl/kg) blunted the aggravation of liver injury observed with the 200 μl dose. This may be due to the redox properties of DMSO, as previously reported (Santos et al., 2003, Sanmartin-Suarez et al., 2011).

The obtained animal data were consistent with the clinico-pathological features of hepatic encephalopathy, indicating that the FHF mouse model was successfully constructed. Importantly, before animal death, hepatic coma developed and lasted for an average of 2 h. Next, we explored the possible mechanisms through which DMSO affected hepatocytes to exacerbate LPS/ᴅ-GalN-induced FHF. Hepatic tissues were injured after treatment with LPS/ᴅ-GalN alone or in combination with DMSO. Further, DMSO co-administration aggravated FHF through increased hepatotoxicity, activation of inflammatory signaling, neutrophil infiltration, hepatocyte apoptosis/necrosis, and nitro-oxidative stress.

Serum levels of AST, ALT, bilirubin, albumin, and urea are the most direct indicators of hepatotoxicity (Jeschke 2009). The increased serum AST, ALT, bilirubin, urea, and low albumin levels in animals 6 h after LPS/ᴅ-GalN injection (10 μg/kg/400 mg/kg) clearly indicated LPS/ᴅ-GalN-caused hepatotoxicity, and these data were in accordance with previously published data (Farghali et al., 2009). DMSO co-administration was found to significantly aggravate hepatotoxicity based on these parameters in LPS/ᴅ-GalN-administrated mice. DMSO co-administration also markedly worsened the histopathological changes induced by LPS/ᴅ-GalN (10 μg/kg/ 400 mg/kg). Histopathological abnormalities were observed 6 h post-injection, characterized by apoptotic/necrotic hepatocytes, inflammatory infiltration, and congested liver sinusoids, all of which were markedly aggravated following DMSO co-administration. Importantly, the survival rate in the DMSO co-administration mice was closely similar to that in the LPS/ᴅ-GalN (10 μg/kg/ 400 mg/kg) group and both were clearly higher than that in the classical LPS/ᴅ-GalN model (50 μg/kg/ 800 mg/kg). These results indicate that DMSO can directly aggravate the hepatotoxic effect of lower dose of the LPS/ᴅ-GalN combination (10 μg/ kg/400 mg/kg), and the use of DMSO can thus be conducive for the study of hepatotoxicity and hepatoprotective compounds using the co-administration model. Therefore, considering that no study had focused on the mechanism(s) through which DMSO exerts its exaggerated effect on LPS/ᴅ-GalN-caused FHF, we set out to determine these.

4.1. DMSO stimulates LPS/ᴅ-GalN-caused FHF by increasing the production of pro-inflammatory cytokine IFN-γ and stimulating STAT1 activation

It is generally accepted that dysregulated inflammatory cytokines expression plays a crucial role in the progression of chronic liver disorders (Szabo and Petrasek 2015). The proinflammatory cytokine IFN-γ is particularly implicated in hepatic damage. IFN-γ is overexpressed in steatohepatitis without infection, driving hepatic inflammation and disease progression (Luo et al., 2013).

Stimulation of the IFN-γ receptor upregulates IRF-1, which acts downstream of the IFN-γ/STAT1 pathway, leading to hepatotoxicity (Kano et al., 1999). Binding of IFN-γ to its receptor causes the phosphorylation of JAK1 and JAK2 (de Weerd and Nguyen 2012). Consequently, STAT1 is recruited to the IFN-γ receptor and is phosphorylated at a tyrosine residue (p-STAT1), resulting in its activation. p-STAT1 then forms a homodimer and is transferred into the cell nucleus to activate a number of genes that promote hepatotoxicity, apoptosis, inflammation, and inhibit hepatic regeneration (Krause et al., 2006, Gao et al., 2012).

To understand the role of IFN-γ in the pathogenesis of hepatic failure caused by LPS/ᴅ-GalN/DMSO treatment, serum level of IFN-γ was examined 2 h after treatment. Our results showed a marked increase in serum IFN-γ levels in LPS/ᴅ-GalN-caused FHF, in harmony with earlier observations (Takano et al., 2009). Co-treatment of DMSO with LPS/ᴅ-GalN resulted in a marked rise in IFN-γ levels compared with LPS/ᴅ-GalN alone. Therefore, DMSO increased liver injury by stimulating IFN-γ production. This observation is consistent with the findings of a previous report by Masson et al. who demonstrated the ability of DMSO to elevate the number of liver NKT cell, activating both NK and NKT cells to release IFN-γ. The authors also found that the pathogenic role of NK and NKT cells in acetaminophen-induced hepatic failure was dependent on the presence of DMSO (Masson et al., 2008).

Since IFN-γ-induced hepatocyte death requires STAT signaling, the activation and expression of STAT1 proteins were assessed 2 h following LPS/ᴅ-GalN/DMSO treatment. Our results presented that p-STAT1 was upregulated 1.6-fold in LPS/ᴅ-GalN-caused FHF and co-injection of DMSO with LPS/ᴅ-GalN induced a highly significant 2.7-fold increase in p-STAT1 level compared to that in control mice and a 2.28-fold increase compared to that in LPS/ᴅ-GalN-injected animals. STAT1 protein expression was only significantly upregulated in the LPS/ᴅ-GalN/DMSO-caused hepatic failure model. In agreement with our results, Kim et al. found that LPS/ᴅ-GalN injection resulted in a peak of p-STAT1 within 4 h, which then reverted to the basal level by 24 h. Furthermore, STAT1 protein expression was significantly increased, starting at 24 h post-injection and lasting for approximately 120 h (Kim et al., 2003). These findings suggest that DMSO may sustain increased levels of IFN-γ and STAT1 by increasing the number of hepatic NKT cells as well as by activating liver NK and NKT cells to secrete more cytotoxic factors that promote liver injury.

4.2. DMSO stimulates LPS/ᴅ-GalN-caused FHF by increasing the production of proinflammatory cytokine TNF-α and stimulating NF-κB activation

At the heart of the complex interplay between hepatocytes and intrahepatic immune cells, are cytokines, particularly TNF-α, which activate immune cells and regulate hepatocyte homeostasis through various intracellular signaling pathways. Kupffer cells are the main sources of TNF-α and IL-6, respectively. The liver tissues are also enriched with NKT and NK cells, which play a role in pathogen defense through IFN-γ production, modulation of hepatic injury, and *T*-cell mobilization (Wahid et al., 2018). TNF-α and related cytokines can influence hepatic cell fate in contrasting manners, acting as pro-apoptotic signals through caspases cascades, but also as antiapoptotic or prosurvival pathway, NF-κB pathway. The signals, where the inactivation of one pathway often depends on the stimulation of another (Baeck and Tacke 2014). In response to bacterial products, such as LPS, large quantities of TNF-α are produced, which can initiate the inflammatory response to liver injury. TNF-α contributes to hepatic inflammation, and prolonged hepatic inflammation leads to hepatic fibrosis, cirrhosis, and, finally, FHF. TNF-α does not cause hepatic damage in normal

hepatic cells *in vivo* due to the strong stimulation of cytoprotective pathways such as the NF-κB pathway. Nevertheless, TNF-α induces hepatotoxicity when the expression of antiapoptotic proteins in the liver is blocked by co-administration of ᴅ-GalN, which mimics disease states (Schwabe and Brenner 2006). In the current study, the observed increase in TNF-α level is in agreement with several reports and confirms the central role TNF-α plays in LPS/ᴅ-GalN-caused FHF (Yang et al., 2016, Jing et al., 2019). Co-treatment with DMSO significantly increased TNF-α levels compared with LPS/ᴅ-GalN administration alone, thus aggravating liver injury through the stimulation of TNF-α production.

LPS-caused TNF-α secretion is regulated by NF-κB in Kupffer cells. Several studies have revealed that NF-κB plays a vital role in LPS/ᴅ-GalN-caused hepatic failure, and its inhibition guards LPS/ᴅ-GalN-treated animals from liver damage (Hu et al., 2018). NF-κB regulates important aspects of liver physiology and pathology. Several toxic stimuli can initiate inflammatory responses by activating NF-κB. PAMPs, in particular LPS, are potent activators of NF-κB signaling, which stimulate TLRs, to then trigger TNF-α secretion. Upon the translocations of NF-κB to the nucleus, various genes containing κB binding sites within their promoters are transcribed, mainly implicated in immune responses and survival (Pahl 1999). The tight regulation of NF-κB at multiple levels is because of the potential danger of uncontrolled inflammation to the host. In unstimulated Kupffer cells, NF-κB families are usually sequestered in the cell cytoplasm, bound to their inhibitors that be a member of the IκB families. Upon cell stimulation in response to specific stimuli, IκB protein is phosphorylated and decomposed by the proteasomes. Consequently, NF-κB enters the cell nucleus and binds DNA, stimulating the transcription of genes encoding inflammatory mediators, including TNF-α, iNOS, and COX-2. Thus, the NF-κB pathways does not act as a survival pathway, but instead can exacerbate liver cell death and hepatic injury (Tak and Firestein 2001, Ashour et al., 2014). To further explore the mechanism(s) through which DMSO exacerbates hepatic injury caused by LPS/ᴅ-GalN, NF-κB levels were quantified by western blot. NF-κB translocations were stimulated by co-treatment with DMSO in LPS/ᴅ-GalN-administrated mice. Therefore, the increase in TNF-α secretion by Kupffer cells may be linked to NF-κB stimulation by DMSO.

4.3. DMSO stimulates LPS/ᴅ-GalN-induced FHF by upregulating apoptosis

Hepatocyte apoptosis drives liver injury in FHF. Programmed cell death is the initial reaction of hepatocytes to a wide range of toxicants (involving endotoxins such as LPS), and necrotic changes in liver cells are often observed after apoptosis. As the central site of detoxification, the liver is continuously exposed to stressors, which disrupt the balance between inflammatory cytokines that stimulate (IFN-γ, TNF-α, IL-12) or inhibit (IL-10, IL-4, MCP-1) liver damage (Nanji et al., 1999). Accordingly, hepatic cells become more sensitive to the harmful effects of the pro-inflammatory cytokines IFN-γ and TNF-α. These bind to intracellular death receptors and consequently stimulate caspase-8. Caspase-8 can initiate programmed cell death *via* direct stimulation of effector caspases-3, 6, and 7 (Wang 2014). Caspase-3 is reflected a key apoptotic "executioner" enzyme in mammals due to its stimulation activates cascades of enzymatic procedures that ends in cell death (Thornberry 1998). Caspase-3 activity was significantly greater in LPS/ᴅ-GalN-treated animals than in the control animals, and DMSO co-administration increased caspase-3 activity relative to that in the LPS/ᴅ-GalN and control groups. Therefore, we concluded that apoptosis was activated by LPS/ᴅ-GalN/DMSO, and this proapoptotic influence may be attributed to the increased produc-

tion of proinflammatory cytokines. Consistent with our results, treatment with LPS/ᴅ-GalN significantly elevated caspase-3 level in mice, as reported in several studies (Wu et al., 2014, Li et al., 2021).

4.4. DMSO stimulates LPS/ᴅ-GalN-caused FHF by increasing COX-2 expression

The expression of various inflammatory molecules, involving COX-2, IL-1β, iNOS, TNF-α and IL-6, is regulated by NF-κB. It has been shown that COX-2 and iNOS activation induce hepatic damage following the nuclear translocation of NF-κB (Luedde and Schwabe 2011). COX-2 produces prostaglandin E2 to mediate cellular proliferation and induces inflammatory processes in various models (Martin-Sanz et al., 2017). In this investigation, LPS/ᴅ-GalN statistically enhanced COX-2 expression in liver tissues by 2.5-fold compared with that in control mice. DMSO co-treatment significantly upregulated COX-2 by 4.4-fold compared to its levels in control mice and 1.7-fold compared to levels in the LPS/ᴅ-GalN treated mice, indicating exaggerated hepatic inflammation. Hence, the DMSO-induced increase in hepatic COX-2 expression may contribute to the exacerbation of hepatic inflammation and damage.

4.5. DMSO stimulates LPS/ᴅ-GalN-induced FHF by increasing neutrophil recruitment

Neutrophil tissue recruitment is a characteristic feature of inflammation. Infiltrating neutrophils induce oxidative damage to liver cells via respiratory burst and degranulation, resulting in massive liver necrosis. TNF-α, mediates neutrophil accumulation in hepatic sinusoids, causing inflammation and hepatocyte death (Maes et al., 2016). Neutrophils contain MPO, which produces hypohalous acid with antimicrobial activity. However, MPO has been shown to cause local tissue damage resulting in inflammation (Aratani 2018). TNF-α causes neutrophil migration in LPS/ᴅ-GalN-caused FHF and plays a crucial role in hepatocyte necrosis (Mohler et al., 1994). Our data demonstrated that LPS/ᴅ-GalN statistically increased MPO activities in liver tissues, while DMSO co-treatment significantly increased MPO activity compared to LPS/ᴅ-GalN alone, indicative of increased hepatic neutrophil infiltration. These data suggest that the DMSO-induced increase in TNF-α production may be linked to the stimulation of neutrophil transmigration.

4.6. DMSO stimulates LPS/ᴅ-GalN-induced FHF by increasing nitro-oxidative stress

Redox imbalances result in nitrosative/oxidative stress, usually as the result of elevated reactive O_2 and N species. Nitrosative and oxidative stress are closely linked to liver dysfunction (Grattagliano et al., 2014). The reaction between NO and O_2^- causes nitrosative stress. The peroxynitrite anion ($ONOO^-$) formed during this process can nitrate numerous biomolecules, such as lipids, proteins, and DNA, to form 3-nitrotyrosine, resulting in lipid peroxidation, cell membrane damage, DNA strand breaks, enzyme inhibition, and the activation of cell death responses (Attia 2010, Jaeschke and Ramachandran 2011). Oxidative/nitrosative stress may underlie the pathophysiology of various hepatic diseases, necessitating its assessment.

NO is a free radical that acts as a cellular signaling molecule in several biochemical processes, synthesized by different NO synthases, including iNOS. Blood vessel contractions are regulated by NO, and high NO levels can limit hepatic cell function or even trigger apoptosis *via* the caspase-independent pathway, mediated through the generation of O_2^- and $^\bullet OH$ intermediates (Langer et al., 2008). Hepatocytes, Kupffer cells, and endothelial cells may

participate in NO production in the liver after exposure to toxic compounds such as LPS. iNOS is a key enzyme that generates NO from the amino acid ʟ-arginine, which plays an important role in inflammation. iNOS is regulated via the NF-κB signalling pathways during inflammatory progression, and improper upregulation or activation of iNOS in response to LPS exposure has drawn considerable attention (Hwang et al., 2017).

We evaluated the influence of DMSO on iNOS and its product, NO (measured as nitrate and nitrite), in LPS/ᴅ-GalN-administered animals. In the current study, there was an upregulation in liver iNOS in LPS/ᴅ-GalN-administered animals, and DMSO co-administration markedly upregulated iNOS, thereby exaggerating hepatic inflammation and damage. Similarly, a significant elevation of hepatic nitrate plus nitrite was obtained after LPS/ᴅ-GalN injection, and co-administration with DMSO induced significantly more nitrate plus nitrite than LPS/ᴅ-GalN alone. These data strongly propose the importance of iNOS and its product NO in the pathogenesis of LPS/ᴅ-GalN-caused FHF, that is in agreement with other results (Yan et al., 2016, Wang et al., 2018). Our data showed that NO formation was enhanced as the result of upregulated iNOS and NF-κB expression, playing an essential role in LPS/ᴅ-GalN/DMSO-caused FHF.

Oxidative cellular stress is closely linked to nitrosative stress. It arises when antioxidant defense systems are overwhelmed, resulting in damage to lipids, proteins, and DNA, in turn causing cell death (Attia 2010, Jaeschke and Ramachandran 2011). Oxidative cellular stress has been proposed to play an important role in the hepatic failure caused by LPS/ᴅ-GalN (Wei et al., 2014). MDA, the end product of lipid peroxidations, is often applied to measure oxidative stress. Our data revealed that LPS/ᴅ-GalN injection significantly elevated MDA level, which is in harmony with earlier results (Yan et al., 2016, Fu et al., 2018). Further, DMSO co-treatment significantly increased LPS/ᴅ-GalN-caused lipid-peroxidation compared with the LPS/ᴅ-GalN alone. Therefore, the toxic impact of DMSO could be attributed to enhancing the oxidative cellular stress caused by LPS/ᴅ-GalN treatment.

Cells counteract oxidative/nitrosative stress through antioxidant defense systems. The antioxidant GSH protects cells against free radicals *via* enzymatic and non-enzymatic reactions. In the present work, a significant reduction in GSH levels was observed following LPS/ᴅ-GalN treatment, which is in harmony with earlier results (Yan et al., 2016, Fu et al., 2018). As expected, LPS/ᴅ-GalN treatment caused notable depletion of liver GSH in animals, which may be linked to LPS/ᴅ-GalN-caused oxidative stress. Co-treatment with DMSO resulted in significantly higher GSH consumption than in LPS/ᴅ-GalN-treated animals. These data propose that DMSO stimulates LPS/ᴅ-GalN-induced hepatic failure by exacerbating the oxidant/antioxidant imbalance.

5. Conclusion

Combinations of LPS/ᴅ-GalN with different doses of DMSO caused significantly greater liver damage than LPS/ᴅ-GalN alone, possibly by upregulating IFN-γ and TNF-α production by hepatocytes to then induce hepatocyte apoptosis and necrosis, liver failure, and death. These findings demonstrate the potential hazard of using DMSO as a solvent in experiments in animal studies. Additionally, the LPS/ᴅ-GalN/DMSO model can be used for the study of hepatotoxicity and pharmacological screening of therapeutics.

Declaration of Competing Interest

The authors declare that they have no known competing financial interests or personal relationships that could have appeared to influence the work reported in this paper.

References

Ahmad, S.F., Zoheir, K.M., Ansari, M.A., et al., 2015. The role of poly(ADP-ribose) polymerase-1 inhibitor in carrageenan-induced lung inflammation in mice. Mol Immunol. 63, 394–405. https://doi.org/10.1016/j.molimm.2014.09.009.

Ahmad, S.F., Nadeem, A., Ansari, M.A., et al., 2017. Upregulation of IL-9 and JAK-STAT signaling pathway in children with autism. Prog Neuropsychopharmacol Biol Psychiatry. 79, 472–480. https://doi.org/10.1016/j.pnpbp.2017.08.002.

Alanazi, A., Algfeley, S.G., Al-Hosaini, K.A., et al., 2017. Therapeutic potential of carfilzomib, an irreversible proteasome inhibitor, against acetaminophen-induced hepatotoxicity in mice. J Biochem Mol Toxicol. 31. https://doi.org/10.1002/jbt.21877.

Al-Hamamah, M.A., Alotaibi, M.R., Ahmad, S.F., et al., 2019. Genetic and epigenetic alterations induced by the small-molecule panobinostat: A mechanistic study at the chromosome and gene levels. DNA Repair (Amst). 78, 70–80. https://doi.org/10.1016/j.dnarep.2019.03.008.

Aratani, Y., 2018. Myeloperoxidase: Its role for host defense, inflammation, and neutrophil function. Arch Biochem Biophys. 640, 47–52. https://doi.org/10.1016/j.abb.2018.01.004.

Ashour, A.E., Abd-Allah, A.R., Korashy, H.M., et al., 2014. Thymoquinone suppression of the human hepatocellular carcinoma cell growth involves inhibition of IL-8 expression, elevated levels of TRAIL receptors, oxidative stress and apoptosis. Mol Cell Biochem. 389, 85–98. https://doi.org/10.1007/s11010-013-1930-1.

Attia, S.M., 2008. Abatement by naringin of lomefloxacin-induced genomic instability in mice. Mutagenesis. 23, 515–521. https://doi.org/10.1093/mutage/gen045.

Attia, S.M., 2010. Deleterious effects of reactive metabolites. Oxid Med Cell Longev. 3, 238–253. https://doi.org/10.4161/oxim.3.4.13246.

Attia, S.M., Al-Anteet, A.A., Al-Rasheed, N.M., et al., 2009. Protection of mouse bone marrow from etoposide-induced genomic damage by dexrazoxane. Cancer Chemother Pharmacol. 64, 837–845. https://doi.org/10.1007/s00280-009-0934-8.

Attia, S.M., Ahmad, S.F., Harisa, G.I., et al., 2013. Wogonin attenuates etoposide-induced oxidative DNA damage and apoptosis via suppression of oxidative DNA stress and modulation of OGG1 expression. Food Chem Toxicol. 59, 724–730. https://doi.org/10.1016/j.fct.2013.07.022.

Attia, S.M., Alshahrani, A.Y., Al-Hamamah, M.A., et al., 2017. Dexrazoxane Averts Idarubicin-Evoked Genomic Damage by Regulating Gene Expression Profiling Associated With the DNA Damage-Signaling Pathway in BALB/c Mice. Toxicol Sci. 160, 161–172. https://doi.org/10.1093/toxsci/kfx161.

Baeck, C., Tacke, F., 2014. Balance of inflammatory pathways and interplay of immune cells in the liver during homeostasis and injury. EXCLI J. 13, 67–81.

Bakheet, S.A., Attia, S.M., Al-Rasheed, N.M., et al., 2011. Salubrious effects of dexrazoxane against teniposide-induced DNA damage and programmed cell death in murine marrow cells. Mutagenesis. 26, 533–543. https://doi.org/10.1093/mutage/ger013.

Bartsch, W., Sponer, G., Dietmann, K., et al., 1976. Acute toxicity of various solvents in the mouse and rat. LD50 of ethanol, diethylacetamide, dimethylformamide, dimethylsulfoxide, glycerine, N-methylpyrrolidone, polyethylene glycol 400, 1,2-propanediol and Tween 20. Arzneimittelforschung. 26, 1581–1583.

Bradley, P.P., Priebat, D.A., Christensen, R.D., et al., 1982. Measurement of cutaneous inflammation: estimation of neutrophil content with an enzyme marker. J Invest Dermatol. 78, 206–209. https://doi.org/10.1111/1523-1747.ep12506462.

de Weerd, N.A., Nguyen, T., 2012. The interferons and their receptors–distribution and regulation. Immunol Cell Biol. 90, 483–491. https://doi.org/10.1038/icb.2012.9.

Ellman, G.L., 1959. Tissue sulfhydryl groups. Arch Biochem Biophys. 82, 70–77. https://doi.org/10.1016/0003-9861(59)90090-6.

Farghali, H., Cerny, D., Kamenikova, L., et al., 2009. Resveratrol attenuates lipopolysaccharide-induced hepatitis in D-galactosamine sensitized rats: role of nitric oxide synthase 2 and heme oxygenase-1. Nitric Oxide. 21, 216–225. https://doi.org/10.1016/j.niox.2009.09.004.

Farghali, H., Kgalalelo Kemelo, M., Wojnarova, L., et al., 2016. In vitro and in vivo experimental hepatotoxic models in liver research: applications to the assessment of potential hepatoprotective drugs. Physiol Res. 65, S417–S425 https://doi.org/10.33549/physiolres.933506.

Fu, T., Li, H., Zhao, Y., et al., 2018. Hepatoprotective effect of alpha-mangostin against lipopolysaccharide/d-galactosamine-induced acute liver failure in mice. Biomed Pharmacother. 106, 896–901. https://doi.org/10.1016/j.biopha.2018.07.034.

Galanos, C., Freudenberg, M.A., Reutter, W., 1979. Galactosamine-induced sensitization to the lethal effects of endotoxin. Proc Natl Acad Sci U S A. 76, 5939–5943. https://doi.org/10.1073/pnas.76.11.5939.

Gama, J.F.G., Cardoso, L., Lagrota-Candido, J.M., et al., 2022. Animal models applied to acute-on-chronic liver failure: Are new models required to understand the human condition? World J Clin Cases. 10, 2687–2699 https://doi.org/10.12998/wjcc.v10.i9.2687.

Gao, B., Wang, H., Lafdil, F., et al., 2012. STAT proteins - key regulators of anti-viral responses, inflammation, and tumorigenesis in the liver. J Hepatol. 57, 430–441. https://doi.org/10.1016/j.jhep.2012.01.029.

Grattagliano, I., Calamita, G., Cocco, T., et al., 2014. Pathogenic role of oxidative and nitrosative stress in primary biliary cirrhosis. World J Gastroenterol. 20, 5746–5759. https://doi.org/10.3748/wjg.v20.i19.5746.

Harisa, G.I., Mariee, A.D., Abo-Salem, O.M., et al., 2014. Erythrocyte nitric oxide synthase as a surrogate marker for mercury-induced vascular damage: the modulatory effects of naringin. Environ Toxicol. 29, 1314–1322. https://doi.org/10.1002/tox.21862.

Hefler, J., Marfil-Garza, B.A., Pawlick, R.L., et al., 2021. Preclinical models of acute liver failure: a comprehensive review. PeerJ. 9, e12579.

Hu, J.J., Wang, H., Pan, C.W., et al., 2018. Isovitexin alleviates liver injury induced by lipopolysaccharide/d-galactosamine by activating Nrf2 and inhibiting NF-kappaB activation. Microb Pathog. 119, 86–92. https://doi.org/10.1016/j.micpath.2018.03.053.

Hwang, J.S., Kwon, M.Y., Kim, K.H., et al., 2017. Lipopolysaccharide (LPS)-stimulated iNOS Induction Is Increased by Glucosamine under Normal Glucose Conditions but Is Inhibited by Glucosamine under High Glucose Conditions in Macrophage Cells. J Biol Chem. 292, 1724–1736. https://doi.org/10.1074/jbc.M116.737940.

Jacob, S.W., Herschler, R., 1986. Pharmacology of DMSO. Cryobiology. 23, 14–27. https://doi.org/10.1016/0011-2240(86)90014-3.

Jaeschke, H., Fisher, M.A., Lawson, J.A., et al., 1998. Activation of caspase 3 (CPP32)-like proteases is essential for TNF-alpha-induced hepatic parenchymal cell apoptosis and neutrophil-mediated necrosis in a murine endotoxin shock model. J Immunol. 160, 3480–3486.

Jaeschke, H., Hasegawa, T., 2006. Role of neutrophils in acute inflammatory liver injury. Liver Int. 26, 912–919. https://doi.org/10.1111/j.1478-3231.2006.01327.x.

Jaeschke, H., Ramachandran, A., 2011. Reactive oxygen species in the normal and acutely injured liver. J Hepatol. 55, 227–228. https://doi.org/10.1016/j.jhep.2011.01.006.

Jaeschke, H., Smith, C.W., 1997. Mechanisms of neutrophil-induced parenchymal cell injury. J Leukoc Biol. 61, 647–653. https://doi.org/10.1002/jlb.61.6.647.

Jeschke, M.G., 2009. The hepatic response to thermal injury: is the liver important for postburn outcomes? Mol Med. 15, 337–351. https://doi.org/10.2119/molmed.2009.00005.

Jing, Z.T., Liu, W., Xue, C.R., et al., 2019. AKT activator SC79 protects hepatocytes from TNF-alpha-mediated apoptosis and alleviates d-Gal/LPS-induced liver injury. Am J Physiol Gastrointest Liver Physiol. 316, G387–G396. https://doi.org/10.1152/ajpgi.00350.2018.

Kano, A., Haruyama, T., Akaike, T., et al., 1999. IRF-1 is an essential mediator in IFN-gamma-induced cell cycle arrest and apoptosis of primary cultured hepatocytes. Biochem Biophys Res Commun. 257, 672–677. https://doi.org/10.1006/bbrc.1999.0276.

Kim, W.H., Hong, F., Radaeva, S., et al., 2003. STAT1 plays an essential role in LPS/D-galactosamine-induced liver apoptosis and injury. Am J Physiol Gastrointest Liver Physiol. 285, G761–G768. https://doi.org/10.1152/ajpgi.00224.2003.

Krause, C.D., He, W., Kotenko, S., et al., 2006. Modulation of the activation of Stat1 by the interferon-gamma receptor complex. Cell Res. 16, 113–123. https://doi.org/10.1038/sj.cr.7310015.

Langer, D.A., Das, A., Semela, D., et al., 2008. Nitric oxide promotes caspase-independent hepatic stellate cell apoptosis through the generation of reactive oxygen species. Hepatology. 47, 1983–1993. https://doi.org/10.1002/hep.22285.

Li, S., Hu, K., Li, L., et al., 2021. Stattic alleviates acute hepatic damage induced by LPS/d-galactosamine in mice. Innate Immun. 27, 201–209. https://doi.org/10.1177/1753425920988330.

Liedtke, C., Trautwein, C., 2012. The role of TNF and Fas dependent signaling in animal models of inflammatory liver injury and liver cancer. Eur J Cell Biol. 91, 582–589. https://doi.org/10.1016/j.ejcb.2011.10.001.

Livak, K.J., Schmittgen, T.D., 2001. Analysis of relative gene expression data using real-time quantitative PCR and the 2(-Delta Delta C(T)). Methods. 25, 402–408. https://doi.org/10.1006/meth.2001.1262.

Luedde, T., Schwabe, R.F., 2011. NF-kappaB in the liver–linking injury, fibrosis and hepatocellular carcinoma. Nat Rev Gastroenterol Hepatol. 8, 108–118. https://doi.org/10.1038/nrgastro.2010.213.

Luo, X.Y., Takahara, T., Kawai, K., et al., 2013. IFN-gamma deficiency attenuates hepatic inflammation and fibrosis in a steatohepatitis model induced by a methionine- and choline-deficient high-fat diet. Am J Physiol Gastrointest Liver Physiol. 305, G891–G899. https://doi.org/10.1152/ajpgi.00193.2013.

Maes, M., Vinken, M., Jaeschke, H., 2016. Experimental models of hepatotoxicity related to acute liver failure. Toxicol Appl Pharmacol. 290, 86–97. https://doi.org/10.1016/j.taap.2015.11.016.

Martin-Sanz, P., Casado, M., Bosca, L., 2017. Cyclooxygenase 2 in liver dysfunction and carcinogenesis: Facts and perspectives. World J Gastroenterol. 23, 3572–3580. https://doi.org/10.3748/wjg.v23.i20.3572.

Masson, M.J., Carpenter, L.D., Graf, M.L., et al., 2008. Pathogenic role of natural killer T and natural killer cells in acetaminophen-induced liver injury in mice is dependent on the presence of dimethyl sulfoxide. Hepatology. 48, 889–897. https://doi.org/10.1002/hep.22400.

Miranda, K.M., Espey, M.G., Wink, D.A., 2001. A rapid, simple spectrophotometric method for simultaneous detection of nitrate and nitrite. Nitric Oxide. 5, 62–71. https://doi.org/10.1006/niox.2000.0319.

Mohler, K.M., Sleath, P.R., Fitzner, J.N., et al., 1994. Protection against a lethal dose of endotoxin by an inhibitor of tumour necrosis factor processing. Nature. 370, 218–220. https://doi.org/10.1038/370218a0.

Nanji, A.A., Jokelainen, K., Rahemtulla, A., et al., 1999. Activation of nuclear factor kappa B and cytokine imbalance in experimental alcoholic liver disease in the rat. Hepatology. 30, 934–943. https://doi.org/10.1002/hep.510300402.

Ohkawa, H., Ohishi, N., Yagi, K., 1979. Assay for lipid peroxides in animal tissues by thiobarbituric acid reaction. Anal Biochem. 95, 351–358. https://doi.org/10.1016/0003-2697(79)90738-3.

Pahl, H.L., 1999. Activators and target genes of Rel/NF-kappaB transcription factors. Oncogene. 18, 6853–6866. https://doi.org/10.1038/sj.onc.1203239.

Robinson, M.W., Harmon, C., O'Farrelly, C., 2016. Liver immunology and its role in inflammation and homeostasis. Cell Mol Immunol. 13, 267–276. https://doi.org/10.1038/cmi.2016.3.

Sanmartin-Suarez, C., Soto-Otero, R., Sanchez-Sellero, I., et al., 2011. Antioxidant properties of dimethyl sulfoxide and its viability as a solvent in the evaluation of neuroprotective antioxidants. J Pharmacol Toxicol Methods. 63, 209–215. https://doi.org/10.1016/j.vascn.2010.10.004.

Santos, N.C., Figueira-Coelho, J., Martins-Silva, J., et al., 2003. Multidisciplinary utilization of dimethyl sulfoxide: pharmacological, cellular, and molecular aspects. Biochem Pharmacol. 65, 1035–1041. https://doi.org/10.1016/s0006-2952(03)00002-9.

Saquib, Q., Attia, S.M., Siddiqui, M.A., et al., 2012. Phorate-induced oxidative stress, DNA damage and transcriptional activation of p53 and caspase genes in male Wistar rats. Toxicol Appl Pharmacol. 259, 54–65. https://doi.org/10.1016/j.taap.2011.12.006.

Sass, D.A., Shakil, A.O., 2005. Fulminant hepatic failure. Liver Transpl. 11, 594–605. https://doi.org/10.1002/lt.20435.

Schlayer, H.J., Laaff, H., Peters, T., et al., 1988. Involvement of tumor necrosis factor in endotoxin-triggered neutrophil adherence to sinusoidal endothelial cells of mouse liver and its modulation in acute phase. J Hepatol. 7, 239–249. https://doi.org/10.1016/s0168-8278(88)80488-4.

Schwabe, R.F., Brenner, D.A., 2006. Mechanisms of Liver Injury. I. TNF-alpha-induced liver injury: role of IKK, JNK, and ROS pathways. Am J Physiol Gastrointest Liver Physiol. 290, G583–G589. https://doi.org/10.1152/ajpgi.00422.2005.

Szabo, G., Petrasek, J., 2015. Inflammasome activation and function in liver disease. Nat Rev Gastroenterol Hepatol. 12, 387–400. https://doi.org/10.1038/nrgastro.2015.94.

Tacke, F., Luedde, T., Trautwein, C., 2009. Inflammatory pathways in liver homeostasis and liver injury. Clin Rev Allergy Immunol. 36, 4–12. https://doi.org/10.1007/s12016-008-8091-0.

Tak, P.P., Firestein, G.S., 2001. NF-kappaB: a key role in inflammatory diseases. J Clin Invest. 107, 7–11. https://doi.org/10.1172/JCI11830.

Takano, H., Inoue, K., Shimada, A., et al., 2009. Urinary trypsin inhibitor protects against liver injury and coagulation pathway dysregulation induced by lipopolysaccharide/D-galactosamine in mice. Lab Invest. 89, 833–839. https://doi.org/10.1038/labinvest.2009.35.

Thornberry, N.A., 1998. Caspases: key mediators of apoptosis. Chem Biol. 5, R97–R. https://doi.org/10.1016/s1074-5521(98)90615-9.

Triantafyllou, E., Woollard, K.J., McPhail, M.J.W., et al., 2018. The Role of Monocytes and Macrophages in Acute and Acute-on-Chronic Liver Failure. Front Immunol. 9, 2948. https://doi.org/10.3389/fimmu.2018.02948.

Wahid, B., Ali, A., Rafique, S., et al., 2018. Role of altered immune cells in liver diseases: a review. Gastroenterol Hepatol. 41, 377–388. https://doi.org/10.1016/j.gastrohep.2018.01.014.

Wang, K., 2014. Molecular mechanisms of hepatic apoptosis. Cell Death Dis. 5, e996.

Wang, W., Wu, L., Li, Q., et al., 2018. Madecassoside prevents acute liver failure in LPS/D-GalN-induced mice by inhibiting p38/NF-kappaB and activating Nrf2/HO-1 signaling. Biomed Pharmacother. 103, 1137–1145. https://doi.org/10.1016/j.biopha.2018.04.162.

Wei, L., Ren, F., Zhang, X., et al., 2014. Oxidative stress promotes D-GalN/LPS-induced acute hepatotoxicity by increasing glycogen synthase kinase 3beta activity. Inflamm Res. 63, 485–494. https://doi.org/10.1007/s00011-014-0720-x.

Wu, Y.H., Hu, S.Q., Liu, J., et al., 2014. Nature and mechanisms of hepatocyte apoptosis induced by D-galactosamine/lipopolysaccharide challenge in mice. Int J Mol Med. 33, 1498–1506. https://doi.org/10.3892/ijmm.2014.1730.

Yan, D., Liu, H.L., Yu, Z.J., et al., 2016. BML-111 Protected LPS/D-GalN-Induced Acute Liver Injury in Rats. Int J Mol Sci. 17. https://doi.org/10.3390/ijms17071114.

Yang, P., Zhou, W., Li, C., et al., 2016. Kupffer-cell-expressed transmembrane TNF-alpha is a major contributor to lipopolysaccharide and D-galactosamine-induced liver injury. Cell Tissue Res. 363, 371–383. https://doi.org/10.1007/s00441-015-2252-2.

Zoheir, K.M., Abd-Rabou, A.A., Harisa, G.I., et al., 2015. Gene expression of IQGAPs and Ras families in an experimental mouse model for hepatocellular carcinoma: a mechanistic study of cancer progression. Int J Clin Exp Pathol. 8, 8821–8831.